Age-related evolution of amyloid burden, iron load, and MR relaxation times in a transgenic mouse model of Alzheimer's disease

Nadine El Tannir El Tayara, Benoit Delatour, Camille Le Cudennec, Maryvonne Guégan, Andreas Volk, Marc Dhenain

Elsevier Editorial System(tm) for Neurobiology of Disease

Manuscript Draft

Manuscript Number: NBD-05-226R2

Title: Age-related evolution of amyloid burden, iron load, and MR relaxation times in a transgenic mouse model of Alzheimer's disease

Article Type: Regular Article

Section/Category:

Keywords: Alzheimer's disease; amyloid; APP; biomarker; iron; MRI; PS1; T1; T2; transgenic mouse

Corresponding Author: Dr. Marc Dhenain, DVM, PhD

Corresponding Author's Institution: Curie Institute

First Author: Nadine El Tannir El Tayara

Order of Authors: Nadine El Tannir El Tayara; Benoît Delatour, PhD; Camille Le Cudennec, PhD; Maryvonne Guégan; Andreas Volk, PhD; Marc Dhenain, DVM, PhD

Manuscript Region of Origin:

Abstract: T1 and T2 magnetic resonance relaxation times have the potential to provide biomarkers of amyloid-β deposition that could be helpful to the development of new therapies for Alzheimer's disease. Here we measured T1 and T2 times as well as plaques and iron loads in APP/PS1 mice, which model brain amyloidosis, and control PS1 mice. Iron was mostly associated with amyloid deposits in APP/PS1 animals, while it was diffuse in the PS1 mice. T1 was negatively correlated with age in most structures in APP/PS1 animals. This may be related to the age-associated myelin loss described in APP/PS1 mice rather than to amyloid deposition. T2 in the subiculum of adult APP/PS1 animals was lower than in PS1 mice, which may be related to the very high amyloid and iron loads in this region. T2 in the subiculum could thus serve as an early marker of the amyloid pathology.

Cover Letter

Institut Curie
La Science au Service de l'Homme
SECTION RECHERCHE

Marc DHENAIN
Laboratoire Raymond LATARJET
Unité 350 de l'INSERM
Biophysique Moléculaire
Bâtiments 112
Centre Universitaire
91405 Orsay Cedex
Tél. (1) 69 86 31 62
Fax (1) 69 07 53 27

Orsay, October, 25th 2005

J.T Greenamyre, MD, PhD
Editor-in-chief
Neurobiology of Disease
University of Pittsburgh
S-506 Biomedical Science Tower
203 Lothrop Street
Pittsburgh, PA 15213
USA

Dear Dr. Greenamyre,

Enclosed, please find our revised manuscript entitled "Age-related evolution of amyloid burden, iron load, and MR relaxation times in a transgenic mouse model of Alzheimer's disease" (NBD-05-226R1). We made appropriate revision in the abstract to provide more conclusive statements as requested by the reviewer.

With best regards.

Marc Dhenain, D.V.M., Ph.D.

*** Response to Reviews**

Response to Reviewer's comments

Reviewer's Question: The article is acceptable pending appropriate revisions of the abstract, replacing vague statements such as " The origin of this modification is discussed ", with more directive conclusive statements. For example, summarizing the relative roles of iron, amyloid or other processes on the MRI parameters observed.

Answer: The sentence "T1 was negatively correlated with age in most structures in APP/PS1 animals. The origin of this modification is discussed" has been replaced by : "T1 was negatively correlated with age in most structures in APP/PS1 animals. This may be related to the age-associated myelin loss described in APP/PS1 mice rather than to amyloid deposition."

Regular Article

Age-related evolution of amyloid burden, iron load, and MR relaxation times in a transgenic mouse model of Alzheimer's disease

Nadine El Tannir El Tayara[1], Benoît Delatour[2], Camille Le Cudennec[2], Maryvonne Guégan[2], Andreas Volk[1], Marc Dhenain[1]

[1] Integrative Imaging Unit; Curie Institute-INSERM, Centre Universitaire. Laboratoire 112, 91405 Orsay Cedex, France.

[2] Laboratoire NAMC, CNRS, UMR 8620, Bât 446, Université Paris Sud, 91405 Orsay, France.

Corresponding author:

Marc Dhenain - Integrative Imaging Unit; Curie Institute-INSERM, Centre Universitaire. Laboratoire 112, 91405 Orsay Cedex, France.

Tel: +33 1 69 86 31 64 ; Fax: +33 1 69 07 53 27

Mail: Marc.Dhenain@curie.u-psud.fr

Abstract:

T1 and T2 magnetic resonance relaxation times have the potential to provide biomarkers of amyloid-β deposition that could be helpful to the development of new therapies for Alzheimer's disease. Here we measured T1 and T2 times as well as plaques and iron loads in APP/PS1 mice, which model brain amyloidosis, and control PS1 mice. Iron was mostly associated with amyloid deposits in APP/PS1 animals, while it was diffuse in the PS1 mice. T1 was negatively correlated with age in most structures in APP/PS1 animals. This may be related to the age-associated myelin loss described in APP/PS1 mice rather than to amyloid deposition. T2 in the subiculum of adult APP/PS1 animals was lower than in PS1 mice, which may be related to the very high amyloid and iron loads in this region. T2 in the subiculum could thus serve as an early marker of the amyloid pathology.

Key words: Alzheimer's disease, amyloid, APP, biomarker, iron, MRI, PS1, T1, T2, transgenic mouse.

Introduction

Alzheimer's disease (AD) is a devastating pathology leading to disastrous cognitive impairments and dementia, associated with major social and economic costs to society. Until now definitive diagnosis required *post mortem* examination of brain tissue, specifically finding evidence of two main neuropathological lesions: senile plaques and neurofibrillary tangles (NFT). These microscopic alterations are mostly distributed in isocortical and hippocampal brain areas. Senile plaques are extracellular deposits of amyloid-β (Aβ) peptides surrounded by dystrophic neurites, while tangles are pathological filaments located in neurons and are mainly made of hyperphosphorylated tau proteins (Jellinger and Bancher, 1998). According to the amyloid cascade hypothesis, it is the accumulation of soluble and insoluble forms of Aβ that constitutes the primary pathogenic event leading to secondary alterations such as NFTs and neuronal death (Hardy and Selkoe, 2002).

Several potential therapies for the disease are currently developed and are being (or will have to be) tested in animal models such as APP or APP/PS1 transgenic mice that overexpress human mutations responsible for familial forms of AD. These genetically modified mice develop extensive Aβ lesions, but no NFTs or marked neuronal loss (but see (Casas et al., 2004)). Such models can therefore be of interest to evaluate the specific effects of Aβ-lowering drugs, which are key to the therapeutic approach today (Dominguez and De Strooper, 2002). The evaluation of these drugs requires availability of *in vivo* biomarkers of the pathology and, for translational studies it would be very helpful to use the same marker in animal and human studies. MRI can be a valuable tool to achieve this goal. MR markers such as temporal brain atrophy contribute to early diagnosis and to follow-up of the disease in humans (Valk et al., 2002). However, atrophy can not be used as a marker of the disease in transgenic mouse models of amyloidosis, because the cerebral atrophy that develops in these mice does not always occur in amyloid-rich cortical areas and is not correlated to the amyloid load (Delatour et al., in press). MR microscopic *post mortem* (Lee et al.,

2004) or *in vivo* (Jack et al., 2004) studies, carried out in transgenic mice, have been successful in detecting cortical Aβ deposits using T2 or T2*-weighted images from aged animals. The plaques appear as dark spots that were presumably caused by the local presence of iron within the amyloid deposits (Falangola et al., 2005b). However, other studies based on T2*-weighted images detected similar spots and iron deposition only in the thalamus but not in other brain structures (Vanhoutte et al., 2005). Studies in human brain samples also reported contradictory results. A study on *post mortem* hippocampi of AD patients showed a detectable T2* effect of the deposits (Benveniste et al., 1999), while another one failed to observe plaque-associated T2* effects in isocortical brain samples (Dhenain et al., 2002). Studies in human samples using T1, T2 (Huesgen et al., 1993), and diffusion–weighted sequences (Benveniste et al., 1999) did not succeed in highlighting individual plaques. Direct detection of individual plaques is indeed a great challenge requiring high spatial resolution at high magnetic field strength, and probably new dedicated contrast agents (Zaim Wadghiri et al., 2003). Alternatively, quantitative assessment of mean relaxation times in regions of interest has the potential to provide indirect markers which can be easily measured in preclinical and clinical settings. However, up to now, studies in humans have led to contradictory results regarding relaxation times modifications in the course of AD. *Post mortem* (Huesgen et al., 1993) or *in vivo* T2 evaluations in the hippocampus or cortical areas of Alzheimer's patients suggested either decrease (Haley et al., 2004), no significant variation (Bondareff et al., 1988), or increase of this parameter (Kirsch et al., 1992; Laakso et al., 1996). *In vivo* studies of gray and white matter T1 relaxation times also reported either no modification, or a T1 increase along the course of the disease (Besson et al., 1985; Christie et al., 1988). Inconsistencies in human studies might come from the co-occurrence of amyloid deposits, NFTs, and associated lesions such as neuronal loss, inflammation, iron deposition, and cerebrospinal fluid (CSF) space dilations leading to partial volume effects on MR images.

To better understand the effect of AD neuropathology on relaxation times it may be useful to focus on transgenic models that mimic mainly one fundamental lesion associated to AD (i.e. Aβ

deposition). A recent study performed at 7 Tesla, has shown a T2 decrease (but no T1 or proton density alterations) in the hippocampus and cingulate (anterior / posterior) cortex of 70-100 week old transgenic mice compared to age-matched non transgenic littermates (Helpern et al., 2004; Falangola et al., 2005a). However no effect could be detected when the APP/PS1 mice were compared to single transgenic PS1 amyloid-deposit free controls (Helpern et al., 2004).

In our study, performed at 4.7 Tesla, T2, T1, and proton density were evaluated in an APP/PS1 mouse model that develops plaques at around 9-14 weeks of age (Blanchard et al., 2003). PS1, amyloid-deposit free, animals were used as controls. More importantly, our cross-sectional study involved animals of a wide age range (27-86 weeks), thus allowing to investigate MR parameters at different stages of amyloid accumulation in the brain. To assess the origin of MRI parameter modifications, the brains were analysed by histology after imaging; both amyloid burden and iron load were assessed.

Materials and methods

Transgenic mice

Transgenic APP/PS1 mice (Thy1 APP751 SL (Swedish mutation KM670/671NL, London mutation V717I introduced in human sequence APP751) x HMG PS1 M146L), modeling early-onset and progressive cerebral amyloid deposition were used (Wirths et al., 2001a; Wirths et al., 2001b; Blanchard et al., 2003). Control animals were amyloid-deposit free PS1 mice. Forty five transgenic mice were evaluated. We distinguished two age groups, “adults” (27 to 45 weeks, 10 APP/PS1, 9 PS1) and “old” animals (60 to 86 weeks, 13 APP/PS1, 13 PS1) for age-matched studies.

MRI experiments and data analysis

In vivo MR images were recorded on a 4.7 Tesla Bruker Biospec 47/30 system, equipped with a 12 cm diameter gradient system (200 mT/m). A surface coil (diameter = 30 mm), actively decoupled from the transmitting birdcage probe (Bruker GmbH) was used for signal acquisition.

Animals were anesthetized with isoflurane (5% for induction, 1-1.5% for maintenance) in a mixture of N_2 (80%) and O_2 (20%) administered via a facemask. Respiration rate was monitored to insure animal stability until the end of the experiment. Body temperature of the mice was maintained by using a water filled heating blanket.

For T2 measurements, a multislice multiecho sequence was used with the following parameters: echo times (TE) = 12.2, 24.4, 36.6, 48.8, 61, 73.2 ms, repetition time (TR) = 2000 ms, field of view (FOV) = 1.5x1.5 cm^2, matrix 128x128, slice thickness = 1 mm, acquisition time = 8min 49s. Five coronal slices equally separated by 2 mm were acquired. They ranged approximately from the frontal lobe to the occipital part of the brain. For the localization of these slices, a horizontal slab of the brain was previously recorded using a fast inversion recovery sequence (TE = 10 ms, TR = 2500 ms, FOV = 3x1.5 cm^2, slice thickness = 9.2 mm, matrix 128x128). On this image, the interventricular foramen, clearly identified, was used as a reference to locate the second slice set.

For T1 measurements, eleven sets of inversion recovery images were recorded by using successively the following inversion times (TI): 13.5, 1500, 100, 800, 500, 1000, 2000, 300, 700, 3000, 900 ms. Imaging parameters were: TE = 10ms, TR = 5000ms, FOV = 1.5x1.5 cm^2, matrix 128x128, slice thickness = 1 mm, total acquisition time (for all the sets) = 1h 57 min. Each set of images comprised three coronal slices equally separated by 2 mm. The first one was located on the interventricular foramen (identified on the image recorded with the fast inversion recovery sequence). The three slices used for T1 measurements had thus the same location as three of the slices used for T2 evaluations. T1 measurements from animals that moved during the inversion recovery acquisitions were discarded from statistical analysis. That was the case of one old APP/PS1 mouse, one adult and three old PS1 mice.

Parametric T1 and T2 maps were generated by fitting pixel intensity values to single exponential curves using the Bruker fit package. Proton density maps were calculated from inversion recovery images after eliminating T2 dependence using the previously calculated T2

maps. Different brain areas were studied: dorsal striatum (caudate/putamen complex), pallidum, thalamus, hippocampus (Ammon's horn), subiculum, parietal and visual cortices, corpus callosum, and temporal muscle (Fig. 1). Regions of interest (ROIs) corresponding to these loci were manually drawn on images acquired with the inversion recovery sequence, for TI=300 or 500 ms. These TI values yielded the best contrast between cerebral structures. The subiculum ROI, which was the smallest one, was placed underneath the cingulum on a slice localized approximately between bregma -2.8 mm and bregma -3.8 mm according to the Paxinos atlas (Paxinos and Franklin, 2001). When this anatomical landmark could not be accurately defined, neither relaxation times, nor proton density were calculated within the subiculum (case of one APP/PS1 mouse and four PS1 animals).

ROI outlines were then transferred to T1, T2, and proton density maps. On T2 maps, additional ROIs were drawn in the frontal cortex. T1, T2, and proton density values were the mean of the ROI drawn on the left and right side of the brain. For each ROI standard deviations (SD) for T1, T2 and proton density were calculated.

Histological analysis

Tissue processing

Following completion of MRI studies, mice were sacrificed by decapitation. The delay between MRI measurements and death was variable from one mouse to the other and only animals sacrificed within 3 weeks following MRI experiments were included in analyses correlating MRI and histological parameters. As reported in the above MRI section, four PS1 animals moved during the inversion recovery image series acquisition and T1 and proton density maps could not be reconstructed for them. Thus for PS1 animals, correlation studies between T1 or proton density measurements and histological markers involved eight animals.

Following decapitation the brains were extracted, fixed in 10 % buffered formalin and then stored overnight in a solution of 20% glycerin and 2% dimethylsulfoxide in 0.1 M phosphate buffer

for cryoprotection. Brains were subsequently sectioned into 40 µm-thick coronal sections on a freezing microtome. Ten batches of serial sections were collected.

Histochemical staining of amyloid plaques

On a first batch of serial sections, ranging from the frontal to the occipital poles, amyloid deposits were labelled by standard Congo red staining (adapted from (Puchtler et al., 1962)). Each slice was then digitized using a Super CoolScan 8000 ED high-resolution scanner (Nikon, Champigny sur Marne, France). Regional amyloid loads (expressed as percent of tissue surface stained by the Congo red dye) were quantified in different brain areas that were previously investigated by means of MRI (parietal and visual cortices, hippocampus, subiculum and thalamus) using computer-based thresholding methods as previously described (Delatour et al., in press). No histological analyses were performed at the level of the striatum, pallidum, and corpus callosum as these brain regions were largely plaque-free.

Histochemical staining of iron

Although biochemical quantification of iron (eg atomic absorption spectrophotometry) is the most valuable and precise method to assess iron concentrations, this approach was discarded as it can not be used to measure iron loads in discrete brain areas. Therefore iron staining was performed on a batch of serial sections using a protocol derived from the standard Perls-DAB method (Nguyen-Legros et al., 1980). Quantification of Perls-stained material has been proven to reflect iron concentrations (Turlin et al., 1992; Masuda et al., 1993) as a linear relationship exists between the two measurements (Masuda et al., 1993). Based on previous work, densitometric analysis of Perls-stained brain tissue was selected to use in the present study (Bizzi et al.,1990; Hill and Switzer, 1984; see below for details).

Briefly, all reactions were carried out on free floating sections to ameliorate tissue penetration of reactives. Blockade of endogenous peroxydase activity was first done by immersion in a methanol/H_20_2 solution. Slices were then treated with equal parts of freshly made, aqueous 2%

potassium ferrocyanide and 2% hydrochloric acid for 20 min. Iron staining was finally intensified using diaminobenzidine (DAB) as chromogen. Brain slices for all PS1 and APP/PS1 mice were simultaneously processed, and incubation in DAB, which was monitored under the microscope to avoid strong background staining, was the same duration for all animals. After staining, slices were mounted on Superfrost plus slides (Fischer Bioblock Scientific, Ilkirch, France), dehydrated and coverslipped for microscopic examination. All slides were digitized as described above under calibrated and constant illumination conditions, and quantification of iron staining intensities was performed using optical density (OD) analysis (see Masuda et al., 1993), which determines levels of iron deposition on the basis of transmitted light in the stained tissue. Analyses of OD were automatically performed in different sampled ROIs (dorsal striatum, corpus callosum, subiculum, parietal cortex) using the Image-Pro Plus software (Media Cybernetics, Silver Spring, USA). The optical density of each pixel was derived from its gray level and mean iron load was defined as the mean OD from all pixels of the ROI. Standards to assess absolute iron quantities were not available for analysis of Perls-stained material (Masuda et al., 1993); therefore only relative quantities of iron deposition were calculated still permiting inter-group comparisons.

Statistical analysis

Statistical analyses using Statistica 6 (StatSoft, Inc., Tulsa, USA) were based on Pearson's, Mann Whitney's, and Wilcoxon's tests. The slopes of the linear regression curves were compared using Student's t-test. The statistical significance level was assigned for $p<.05$.

Results

Histology

Amyloid load in APP/PS1 mice

We found a positive linear correlation between age and amyloid burden in all sampled brain areas of APP/PS1 mice (Fig. 2, $rs>0.51$; $ps<.025$). Regional amyloid loads were inter-correlated

(rs>0.74; ps<.001) with the highest mean load at each age occurring in the subiculum area (Fig. 2; for adult animals subicular amyloid load = 8.9±1.6 (mean±SD) versus amyloid loads < 3.9± 1.8 in other brain regions (Wilcoxon's tests, ps< 0.03); for old animals subicular amyloid load = 13.6±6.1 versus amyloid loads < 7.5±2.5 in other brain regions (Wilcoxon's tests, ps< 0.001)).

Iron deposition in APP/PS1 and PS1 mice

Qualitative examination of Perls-DAB-stained brain sections revealed that in both APP/PS1 and PS1 genotypes iron deposition was more pronounced in subcortical nuclei (caudate nucleus, pallidum, substantia nigra, thalamus) and in fiber tracts (e.g. corpus callosum, internal capsule) than in other brain structures such as cortical regions (Fig. 3a-d). For APP/PS1 mice, iron in brain regions with amyloid deposits (cortex, subiculum, hippocampus, thalamus) was often localized within the amyloid deposits, whereas in the same regions of PS1 animals iron was diffusely distributed (Fig. 3e-h). By visual inspection, the density of plaque-associated iron aggregates in APP/PS1 mice was much higher in the subiculum (Fig. 3e) than in isocortical regions (Fig. 3g). Quantification of iron by optical densitometry confirmed this observation; the mean iron load in the subiculum of APP/PS1 mice was higher than in the cortex (Wilcoxon's tests; p<0.0005). Indeed, it was similar to that in brain regions known for their high iron load, such as the corpus callosum or the striatum (Wilcoxon's tests; ns). Furthermore, in the subiculum a positive correlation was observed between amyloid deposits and mean iron load (r= 0.5; p<.05) (Fig. 4). This was not the case for brain regions with lower amyloid burden, such as the parietal cortex (r= 0.15; ns) (Fig. 4).

In most brain regions (corpus callosum, parietal cortex, subiculum), despite a positive trend there was no statistically significant increase of mean iron load with aging, neither in APP/PS1 (rs < 0.41; ns) nor in PS1 (rs < 0.3; ns) transgenics. A positive correlation between age and mean iron load was detected in the dorsal striatum of APP/PS1 (r=0.64; p<.005), but not in PS1 mice (r=0.39; ns).

Comparison of mean iron load for the two genotypes showed no differences for adult mice (Us>7; ns). In old mice the same analysis indicated only an effect of genotype in the parietal cortex, where PS1 mice showed increased iron load compared to APP/PS1 mice (U=25.5; p<.025).

Intra-genotype analysis indicated that iron loads were systematically inter-correlated in PS1 mice (.0001<ps<.025), indicating that variations of iron loads equally affected all brain regions in those control animals. In APP/PS1 mice a more complex pattern was noted, as only iron loads in the corpus callosum and dorsal striatum were positively correlated (r= 0.53; p<.025). This suggests that iron deposition may not be a homogeneous process in double transgenics, and could differentially affect several brain areas.

MRI parameters and histological correlates

Effects of aging on MRI parameters

In both genotypes, **T2** values from all the brain regions and the muscle were linearly and negatively correlated to age (Table 1, Fig. 5a, b). For a given genotype, the rate of T2 decrease with aging was similar for all brain regions, as shown by comparable slopes of the regression curves fitting T2 values versus age in the different ROIs (t-tests comparing the slopes of these regression curves; ns).

Striatal **T1** values and age were linearly and negatively correlated in both APP/PS1 and PS1 mice (Table 1, Fig. 6a), and the age-dependent decay of striatal T1 was similar in the two genotypes (t-test comparing the slopes of the regression curves; ns). In addition, in APP/PS1 mice only, negative correlations between T1 values and age were also found in the corpus callosum, the thalamus, the parietal cortex (Fig. 6b) and the pallidum (see Table 1). In these animals, the T1 decay with aging was significantly faster in the corpus callosum than in the thalamus, striatum and parietal cortex (t-tests comparing the slopes of the regression curves fitting T1 values as a function of age; ps<.05).

In both genotypes, **proton density** values were not correlated with age.

T2, T1 and proton density differences between genotypes

T2 values in the subiculum of adult APP/PS1 animals were significantly lower than those of age-matched PS1 mice (Mann Whitney's test, U=8.5, $n_{APP/PS1}$=10 and n_{PS1}=7; p<.01, Fig. 7). In contrast, in aged animals subicular T2 was not significantly different between APP/PS1 and PS1 mice (Mann Whitney's test, U=61.5, $n_{APP/PS1}$=12 and n_{PS1}=11; ns). No other T2 differences between APP/PS1 and PS1 animals could be detected in adult or old age-matched animals (Us>22; ns). When comparing slopes of T2 versus age regressions from the two genotypes, a significant difference was only observed in the subiculum. In this region, the slope for APP/PS1 animals was lower than that for PS1 mice (t-test, p<.05).

Comparison of **T1** values in APP/PS1 and PS1 age-matched animals showed significantly lower T1 in the corpus callosum and the parietal cortex of old APP/PS1 mice (Us<13; ps<.01). No other difference could be detected between age-matched animals from the two genotypes.

Comparison of **proton density** values did not show any significant difference between the age-matched groups.

Effects of plaque burden on MRI parameters

In all the brain regions studied, **T2** measures in APP/PS1 transgenic mice were negatively correlated with the corresponding amyloid load (Table 1). The slope of the regression curve fitting T2 versus regional amyloid load was significantly lower in the subiculum than in the hippocampus (p<.01), the parietal cortex (p<.05), and the visual cortex (p<.01).

T1 values and regional amyloid loads were negatively correlated in isocortical areas (parietal, visual cortices) but not at the level of the subiculum, hippocampus, and the thalamus (Table 1).

Finally, **proton density** measures were not affected by the amyloid load in APP/PS1 transgenic mice.

Effects of iron on MRI parameters

In APP/PS1 and PS1 animals, there was no correlation between the mean iron load in the parietal cortex, subiculum, or corpus callosum and **T2 or T1** values in the same regions (see Table 1). For APP/PS1 mice only, a strong negative correlation was noted between striatal iron and T2 or T1 (Table 1).

There was no correlation between **proton density** values and iron deposition in the different sampled brain areas from PS1 and APP/PS1 mice.

Discussion

Proton density, T2 and T1 relaxation times were evaluated, together with histological parameters, during a cross-sectional study involving a large number (n=45) of APP/PS1 mice modelling amyloid deposit, and PS1 amyloid-deposit free animals. The use of PS1 animals as controls allowed us to specifically assess the effects of amyloid deposition on MR parameters.

Histological measures revealed, as expected (Blanchard et al., 2003), an age–related increase of the amyloid load in all the evaluated regions (cortex, hippocampus, thalamus, subiculum). However, mean iron loads did not increase with age except in the dorsal striatum of APP/PS1 mice. In several animal species, cerebral iron (evaluated by chemical method in humans (Hallgren and Sourander, 1958) or by atomic emission spectrometry in mice (Takahashi et al., 2001)) increases in the early period of life and reaches a plateau in mature and old adults. In our study, the lack of age-related iron accumulation in most brain regions (in 27-83 week old animals) might be related to the fact that iron level already had reached a plateau which normally occurs at 17 weeks in mice (Takahashi et al., 2001).

In amyloid-rich regions (subiculum, cortex, hippocampus, and thalamus) of APP/PS1 mice iron staining was colocalized, to a large extent, with amyloid deposits whereas in the same brain loci it was diffuse in PS1 mice. The colocalization of iron and amyloid deposits observed in our study replicates previous findings reported in the literature (Falangola et al., 2005b). In addition, we

noticed that, in most brain regions, despite a different spatial distribution, the mean iron load was similar in age-matched APP/PS1 and PS1 mice. This suggests that iron aggregated within the plaques comes from the diffuse iron that is normally located in the tissues. Moreover, in the parietal cortex, the mean iron load was even lower in APP/PS1 than in PS1 animals. These results are coherent with previous reports that showed, on whole brain samples assessed by spectrometry, a reduced (or not modified) cerebral iron load in other transgenic mouse models of AD (Maynard et al., 2002). They are also consistent with findings suggesting that Aβ deposits can clear iron out of the brain (Maynard et al., 2002; Bush, 2003).

A linear relationship between mean iron load and amyloid load could be detected in the subiculum of APP/PS1 mice (the brain region with the highest plaque density) but not in the cortex. This suggests that amyloid biomarkers based on iron load are more reliable in the subiculum than in other brain regions such as the cortex. This has implication for direct amyloid deposit imaging by microscopic MRI without contrast agents. Since in this method amyloid detection and quantification are based on the presence of iron within the plaques (Jack et al., 2004), it should yield more accurate results for the subiculum than for the cortex.

In brain structures with amyloid deposits, T2 and amyloid load were correlated in APP/PS1 mice. However, amyloid load increased with age and T2 and age were also correlated in all the studied brain regions in both APP/PS1 and PS1 mice. In addition, except in the subiculum the slopes of the regression curves fitting T2 and age were similar in APP/PS1 and PS1 animals. Finally, T2 values from age-matched APP/PS1 and PS1 animals were not significantly different. This suggests that in most brain structures (but not the subiculum, see below), age related effects other than amyloid deposition were the main factors in the age-related T2 decrease. This is consistent with reports from a previous transversal study in 70-100 week old APP/PS1 and PS1 animals, where no inter-genotype T2 differences could be detected in the cingulate and retrosplenial cortex or the hippocampus (Helpern et al., 2004). Interestingly however, data from the same study showed T2 differences in the cortex and hippocampus of APP/PS1 (but not PS1) animals with

respect to wild-type mice. This suggests an additive but amyloid independent effect of double APP and PS1 transgene expression on cortical T2 relaxation times. As we used only PS1 mice as controls, we could not examine this effect.

Iron is often evoked to explain age-related T2 signal decrease in the brain (Dhenain et al., 1998; Hardy et al., 2005). However, from the lack of correlation between mean iron load and T2 or age in most of the evaluated brain regions (both in APP/PS1 and PS1), it seems that iron did not participate significantly in the age-related T2 decrease observed in our study. This T2 decrease might be associated with already described age-related brain alterations such as increased brain density and reduced free water content (Lustyik and Nagy, 1985; Chang et al., 1996), and/or to changes in intracellular or extracellular environments leading to decreased water mobility (Bondareff and Narotzky, 1972).

Unlike in other brain structures, the T2 in the subiculum of adult APP/PS1 animals was significantly lower than in adult PS1 mice. To our knowledge, this is the first report showing a significant T2 difference in a brain region between APP/PS1 and PS1 mice. The mean iron load in the subiculum of APP/PS1 mice was higher than in any other amyloid enriched region, and in the subiculum the iron and amyloid loads were correlated. Previous reports showed that iron clusters lead to a larger T2 decrease than diffuse forms of iron (Perez et al., 2002). In our study, where the mean iron load was not significantly different between adult APP/PS1 and PS1 mice, it is possible that the dense aggregation of iron in the subiculum of APP/PS1 mice led to the lower T2 in contrast to diffuse iron distribution in PS1 mice. In addition, the T2 decrease in the subiculum of APP/PS1 as compared to PS1 mice might also be explained by the high amyloid load in this region and its early onset during ontogenesis (Blanchard et al., 2003). The high level of misfolded, ß sheeted amyloid proteins in the extracellular space might reduce water mobility and thus T2. Unexpectedly, in older animals there was no subicular T2 difference between PS1 and APP/PS1 animals. This lack of difference is explained by a slower age-associated subicular T2 decrease in APP/PS1 as compared to PS1 mice. As mean iron load is similar in aged APP/PS1 and PS1 mice this might be

caused by secondary neuropathological alterations in this region (that may or not be associated with long lasting and severe amyloidosis) leading to a T2 increase that partly compensates for the amyloid/iron associated T2 decrease. This hypothesis is favoured by the lower slope of the regression curve fitting T2 versus regional amyloid load in the subiculum as compared to other amyloid-loaded regions (hippocampus, parietal cortex, visual cortex). It has to be noted that the counteracting effects on T2 relaxation must occur on a sub-voxel scale, as the standard deviation of the T2 measured in the subiculum ROI was not modified in old APP/PS1 (data not shown). Inflammation is described in APP/PS1 mice (Matsuoka et al., 2001) and is associated with extracellular space expansion (Stanisz et al., 2004) and might be responsible for the suspected T2 increase. Alternatively, neuronal alterations have also been suggested as a cause for T2 increase in AD patients (Bondareff et al., 1988; Kirsch et al., 1992) and might lead to a T2 increase in old APP/PS1 mice who are known to develop neuronal alterations (Schmitz et al., 2004).

T1 values were significantly lower in the parietal cortex and corpus callosum of aged APP/PS1 as compared to age-matched PS1 mice. This result is different from that reported in a previous study at 7 Tesla where no T1 difference could be seen between APP/PS1, PS1 and wild type animals (Helpern et al., 2004). As T1 contrast decreases with higher field strength, it is possible that T1 differences are better detected at our lower field (4.7 Tesla). The strong correlation identified between the T1 decrease and amyloid deposition in parietal and visual cortices of APP/PS1 mice would suggest that T1 reduction in cortical regions is tightly associated with local amyloid pathology. However, in other brain regions with high amyloid burden such as the subiculum and the hippocampus, amyloid load and T1 were not correlated. Analysis of age-related T1 decrease in our study can provide an alternative hypothesis to explain the T1 decrease in the cortex of APP/PS1 mice. Actually, T1 measures in APP/PS1 mice were correlated to age in all subcortical structures (thalamus, striatum, pallidum), in the corpus callosum, and in the parietal (but not visual) cortex. This suggests that age-related T1 reductions occurred in brain regions both with or without amyloid deposits.

In all evaluated structures, except the striatum, from PS1 animals, T1 measures were not correlated with age. The specific age-related T1 reductions in APP/PS1 mice were not related to iron accumulation as in most of these regions T1 and iron load were not correlated, and in the age window we studied we saw no age-related iron accumulation. In some studies (but see Baratti et al., 1999), T1 reductions in brain tissue have been associated with demyelination (Parry et al., 2003). In a previous study, we demonstrated that APP/PS1 mice show white matter alterations (Delatour et al., in press); it is thus possible that the age-related T1 decrease found in several brain structures from APP/PS1 mice was related to white matter loss. This hypothesis can also explain the T1 decrease in the cortex as in this region the myeloarchitecture strongly affects the T1 signal (Eickhoff et al., 2005).

In conclusion, our histological analysis showed that in amyloid-rich regions such as the cortex or subiculum of APP/PS1 mice, iron accumulates in amyloid plaque-associated forms, while in PS1 mice the iron distribution is diffuse. However, the global iron content in these regions is not higher in APP/PS1 animals as compared to PS1 mice. This suggests that iron accumulation within the plaques results from a redistribution of surrounding diffuse iron rather than from additional iron trapping. Our MRI study showed that T2 is lower in the subiculum of adult APP/PS1 animals as compared to PS1 mice. T2 in the subiculum could thus be considered as an early marker of the amyloid pathology in APP/PS1 animals. The high amyloid and amyloid-associated iron loads in the subiculum of APP/PS1 mice might explain the specific T2 changes in this structure. The disappearance of T2 difference in the subiculum of old APP/PS1 and PS1 mice might be related to a concurrent T2 increase in APP/PS1 animals as a result of pathological modifications associated (or not) to the high amyloid burden. The second result from the MRI study concerns the specific age-related T1 decrease in several brain structures from APP/PS1 mice independent of their amyloid load. Both observations, provided by T2 and T1 measurements, may be useful to follow neuropathological alterations in APP/PS1 models of Alzheimer's disease.

Acknowledgements

We thank the Sanofi-Aventis Neurodegenerative Disease Group for the generous gift of the animals involved in this study and Dr. Libbey for reading and correcting this manuscript. This work was supported by the Aging ATC 2002 (INSERM), the Fédération pour la Recherche sur le Cerveau 2003, the Del Duca Foundation, and the ACI Neurosciences 2004 (French Research Department).

References

Baratti, C., Barnett, A.S., Pierpaoli, C., 1999. Comparative MR imaging study of brain maturation in kittens with T1, T2, and the trace of the diffusion tensor. Radiology. 210, 133-142.

Benveniste, H., Einstein, G., Kim, K.R., Hulette, C., Johnson, G.A., 1999. Detection of neuritic plaques in Alzheimer's disease by magnetic resonance microscopy. P. Natl. Acad. Sci. USA. 96, 14079-14084.

Besson, J.A., Corrigan, F.M., Foreman, E.I., Eastwood, L.M., Smith, F.W., Ashcroft, G.W., 1985. Nuclear magnetic resonance (NMR). II. Imaging in dementia. Br. J. Psychiatry. 146, 31-35.

Bizzi, A., Brooks, R.A., Brunetti, A., Hill, J.M., Alger, J.R., Miletich, R.S., Francavilla, T.L., Di Chiro, G., 1990. Role of iron and ferritin in MR imaging of the brain: A study in primates at different field strengths. Radiology. 177, 59-65.

Blanchard, V., Moussaoui, S., Czech, C., Touchet, N., Bonici, B., Planche, M., Canton, T., Jedidi, I., Gohin, M., Wirths, O., Bayer, T.A., Langui, D., Duyckaerts, C., Tremp, G., Pradier, L., 2003. Time sequence of maturation of dystrophic neurites associated with Ab deposits in APP/PS1 transgenic mice. Exp. Neurol. 184, 247-263.

Bondareff, W., Narotzky, R., 1972. Age changes in the neuronal microenvironment. Science. 176, 1135-1136.

Bondareff, W., Raval, J., Colletti, P.M., Hauser, D.L., 1988. Quantitative magnetic resonance imaging and the severity of dementia in Alzheimer's disease. Am. J. Psychiatry. 145, 853-856.

Bush, A.I., 2003. The metallobiology of Alzheimer's disease. Trends Neurosci. 26, 207-214.

Casas, C., Sergeant, N., Itier, J.M., Blanchard, V., Wirths, O., van der Kolk, N., Vingtdeux, V., van de Steeg, E., Ret, G., Canton, T., Drobecq, H., Clark, A., Bonici, B., Delacourte, A., Benavides, J., Schmitz, C., Tremp, G., Bayer, T.A., Benoit, P., Pradier, L., 2004. Massive CA1/2 neuronal loss with intraneuronal and N-terminal truncated Abeta42 accumulation in a novel Alzheimer transgenic model. Am. J. Pathol. 165, 1289-1300.

Chang, L., Ernst, T., Poland, R.E., Jenden, D.J., 1996. In vivo proton magnetic resonance spectroscopy of the normal aging human brain. Life Sci. 58, 2049-2056.

Christie, J.E., Kean, D.M., Douglas, R.H., Engleman, H.M., St Clair, D., Blackburn, I.M., 1988. Magnetic resonance imaging in pre-senile dementia of the Alzheimer-type, multi-infarct dementia and Korsakoff's syndrome. Psychol. Med. 18, 319-329.

Delatour, B., Guegan, M., Volk, A., Dhenain, M., in press. In vivo MRI and histological evaluation of brain atrophy in APP/PS1 transgenic mice. Neurobiol. Aging.2005 Jul 14. [Epub ahead of print]

Dhenain, M., Duyckaerts, C., Michot, J.-L., Volk, A., Picq, J.-L., Boller, F., 1998. Cerebral T2-weighted signal decrease during aging in the mouse lemur primate reflects iron accumulation. Neurobiol. Aging. 19, 65-69.

Dhenain, M., Privat, N., Duyckaerts, C., Jacobs, R.E., 2002. Senile plaques do not induce susceptibility effects in T2*-weighted MR microscopic images. NMR Biomed. 15, 197-203.

Dominguez, D.I., De Strooper, B., 2002. Novel therapeutic strategies provide the real test for the amyloid hypothesis of Alzheimer's disease. Trends Pharmacol Sci. 23, 324-330.

Eickhoff, S., Walters, N.B., Schleicher, A., Kril, J., Egan, G.F., Zilles, K., Watson, J.D., Amunts, K., 2005. High-resolution MRI reflects myeloarchitecture and cytoarchitecture of human cerebral cortex. Hum. Brain Mapp. 24, 206-215.

Falangola, M.F., Ardekani, B.A., Lee, S.P., Babb, J.S., Bogart, A., Dyakin, V.V., Nixon, R., Duff, K., Helpern, J.A., 2005a. Application of a non-linear image registration algorithm to quantitative analysis of T2 relaxation time in transgenic mouse models of AD pathology. J. Neurosci. Methods. 144, 91-97.

Falangola, M.F., Lee, S.P., Nixon, R.A., Duff, K., Helpern, J.A., 2005b. Histological co-localization of iron in Abeta plaques of PS/APP transgenic mice. Neurochem. Res. 30, 201-205.

Haley, A.P., Knight-Scott, J., Fuchs, K.L., Simnad, V.I., Manning, C.A., 2004. Shortening of hippocampal spin-spin relaxation time in probable Alzheimer's disease: a 1H magnetic resonance spectroscopy study. Neurosci. Lett. 362, 167-170.

Hallgren, B., Sourander, P., 1958. The effect of age on the non-haemin iron in the human brain. J. Neurochem. 3, 41-55.

Hardy, J., Selkoe, D.J., 2002. The amyloid hypothesis of Alzheimer's disease: progress and problems on the road to therapeutics. Science. 297, 353-356.

Hardy, P.A., Gash, D., Yokel, R., Andersen, A., Ai, Y., Zhang, Z., 2005. Correlation of R2 with total iron concentration in the brains of rhesus monkeys. J. Magn. Reson. Imaging. 21, 118-127.

Helpern, J.A., Lee, S.P., Falangola, M.F., Dyakin, V.V., Bogart, A., Ardekani, B., Duff, K., Branch, C., Wisniewski, T., de Leon, M.J., Wolf, O., O'Shea, J., Nixon, R.A., 2004. MRI assessment of neuropathology in a transgenic mouse model of Alzheimer's disease. Magn. Reson. Med. 51, 794-798.

Hill, J.M., Switzer, R.C., 1984. The regional distribution and cellular localization of iron in the rat brain. Neuroscience. 11, 595-603.

Huesgen, C.T., Burger, P.C., Crain, B.J., Johnson, G.A., 1993. In vitro MR microscopy of the hippocampus in Alzheimer's disease. Neurology. 43, 145-152.

Jack, C.R., Jr., Garwood, M., Wengenack, T.M., Borowski, B., Curran, G.L., Lin, J., Adriany, G., Grohn, O.H., Grimm, R., Poduslo, J.F., 2004. In vivo visualization of Alzheimer's amyloid plaques by magnetic resonance imaging in transgenic mice without a contrast agent. Magn. Reson. Med. 52, 1263-1271.

Jellinger, K.A., Bancher, C., 1998. Neuropathology of Alzheimer's disease: a critical update. J. Neural. Transm. Suppl. 54, 77-95.

Kirsch, S.J., Jacobs, R.W., Butcher, L.L., Beatty, J., 1992. Prolongation of magnetic resonance T2 time in hippocampus of human patients marks the presence and severity of Alzheimer's disease. Neurosci. Lett. 134, 187-190.

Laakso, M.P., Partanen, K., Soininen, H., Lehtovirta, M., Hallikainen, M., Hanninen, T., Helkala, E.L., Vainio, P., Riekkinen, P.J., Sr., 1996. MR T2 relaxometry in Alzheimer's disease and age-associated memory impairment. Neurobiol. Aging. 17, 535-540.

Lee, S.P., Falangola, M.F., Nixon, R.A., Duff, K., Helpern, J.A., 2004. Visualization of beta-Amyloid Plaques in a Transgenic Mouse Model of Alzheimer's Disease Using MR Microscopy Without Contrast Reagents. Magn. Reson. Med. 52, 538-544.

Lustyik, G., Nagy, I., 1985. Alterations of the intracellular water and ion concentrations in brain and liver cells during aging as revealed by energy dispersive X-ray microanalysis of bulk specimens. Scan. Electron. Microsc. 323-337.

Masuda, T., Kasai, T., Satodate, R., 1993. Quantitative measurement of hemosiderin deposition in tissue sections of the liver by image analysis. Anal. Quant. Cytol. Histol. 15,379-382.

Matsuoka, Y., Picciano, M., Malester, B., LaFrancois, J., Zehr, C., Daeschner, J.M., Olschowka, J.A., Fonseca, M.I., O'Banion, M.K., Tenner, A.J., Lemere, C.A., Duff, K., 2001. Inflammatory responses to amyloidosis in a transgenic mouse model of Alzheimer's disease. Am. J. Pathol. 158, 1345-1354.

Maynard, C.J., Cappai, R., Volitakis, I., Cherny, R.A., White, A.R., Beyreuther, K., Masters, C.L., Bush, A.I., Li, Q.X., 2002. Overexpression of Alzheimer's Disease Amyloid-beta Opposes the Age- dependent Elevations of Brain Copper and Iron. J. Biol. Chem. 277, 44670-44676.

Nguyen-Legros, J., Bizot, J., Bolesse, M., Pulicani, J.-P., 1980. "Noir de diaminobenzidine" : une nouvelle méthode histochimique de révélation du fer exogène ("Diaminobenzidine black": A new histochemical method for the visualization of exogenous iron). Histochemistry. 66, 239-244.

Parry, A., Clare, S., Jenkinson, M., Smith, S., Palace, J., Matthews, P.M., 2003. MRI brain T1 relaxation time changes in MS patients increase over time in both the white matter and the cortex. J. Neuroimaging. 13, 234-239.

Paxinos, G., Franklin, K.B.J., 2001. The mouse brain in stereotaxic coordinates. Academic Press, San Diego.

Perez, J.M., Josephson, L., O'Loughlin, T., Hogemann, D., Weissleder, R., 2002. Magnetic relaxation switches capable of sensing molecular interactions. Nat. Biotechnol. 20, 816-820.

Puchtler, H., Sweat, F., Levine, M., 1962. On the binding of Congo red by amyloid. J. Histochem. Cytochem. 10, 355-364.

Schmitz, C., Rutten, B.P., Pielen, A., Schafer, S., Wirths, O., Tremp, G., Czech, C., Blanchard, V., Multhaup, G., Rezaie, P., Korr, H., Steinbusch, H.W., Pradier, L., Bayer, T.A., 2004. Hippocampal neuron loss exceeds amyloid plaque load in a transgenic mouse model of Alzheimer's disease. Am. J. Pathol. 164, 1495-1502.

Stanisz, G.J., Webb, S., Munro, C.A., Pun, T., Midha, R., 2004. MR properties of excised neural tissue following experimentally induced inflammation. Magn. Reson. Med. 51, 473-479.

Takahashi, S., Takahashi, I., Sato, H., Kubota, Y., Yoshida, S., Muramatsu, Y., 2001. Age-related changes in the concentrations of major and trace elements in the brain of rats and mice. Biol. Trace. Elem. Res. 80, 145-158.

Turlin, B., Loreal, O., Moirand, R., Brissot, P., Deugnier, Y., Ramee, M.P., 1992. Détection histochimique du fer hépatique. Etude comparative de quatre colorations. Ann. Pathol. 12, 371-373. [Histochemical detection of hepatic iron. A comparative study of four stains].

Valk, J., Barkhof, F., Scheltens, P., 2002. Magnetic Resonance in Dementia. Springer-Verlag, Heidelberg Berlin New York.

Vanhoutte, G., Dewachter, I., Borghgraef, P., Van Leuven, F., Van der Linden, A., 2005. Noninvasive in vivo MRI detection of neuritic plaques associated with iron in APP[V717I] transgenic mice, a model for Alzheimer's disease. Magn. Reson. Med. 53, 607-613.

Wirths, O., Multhaup, G., Czech, C., Blanchard, V., Moussaoui, S., Tremp, G., Pradier, L., Beyreuther, K., Bayer, T.A., 2001a. Intraneuronal Abeta accumulation precedes plaque formation in beta-amyloid precursor protein and presenilin-1 double-transgenic mice. Neurosci. Lett. 306, 116-120.

Wirths, O., Multhaup, G., Czech, C., Blanchard, V., Tremp, G., Pradier, L., Beyreuther, K., Bayer, T.A., 2001b. Reelin in plaques of beta-amyloid precursor protein and presenilin-1 double-transgenic mice. Neurosci. Lett. 316, 145-148.

Zaim Wadghiri, Y., Sigurdsson, E.M., Sadowski, M., Elliott, J.I., Li, Y., Scholtzova, H., Tang, C.Y., Aguilnaldo, G., Pappolla, M., Duff, K., Wisniewski, T.M., Turnbull, D.H., 2003. Detection of Alzheimer's amyloid in transgenic mice using magnetic resonance microimaging. Magn. Reson. Med. 50, 293-302.

Table and Figures

Table 1

Overview of correlations between MRI measures (T2, T1) and histological markers (iron and regional amyloid loads) in different brain areas from APP/PS1 and PS1 mice. *: p <,05; **: p <,01; ***: p <,001; na: non-assessed; ns: non-significant.

Figure 1

Regions of interest on images acquired with an inversion recovery sequence. (a): 1 and 2: muscle, 3 and 4: dorsal striatum (caudate/putamen), 5 and 6: pallidum; (b): 7 and 8: hippocampus, 9 and 10: thalamus, 11 and 12: parietal cortex, 13: corpus callosum; (c): 14 and 15: subiculum, 16 and 17: visual cortex. Scale bar : 700 µm

Figure 2

Correlation between amyloid load and age in various brain regions from APP/PS1 animals (a). Regression curves fitting amyloid and age were drawn for each region (▲, ·····: hippocampus, r=0.7; ◊, ——: parietal cortex, r= 0.8, □, ——: thalamus, r=0.8, ♦, ····· : subiculum, r=0.5). At any age, the amyloid load was higher in the subiculum than in other brain regions. Congo-red stained histological sections showing the parietal cortex and the subiculum for adult (29 weeks; b) and old (83 weeks; c) mice. Note the high amyloid burden in the subiculum (arrows), even in adult mice (b). Scale bar (for b and c): 2 mm.

Figure 3

Iron deposition in adult (29 weeks, a, c) and old (77 weeks, b, d) PS1 and APP/PS1 mice (Perls-DAB staining). (a-d) Note the high iron staining at the level of the striatum (*) and fiber tracts such as the anterior commissure (arrow head) and the corpus callosum (arrow). Perls-DAB staining also showed iron deposits in the vicinity of subicular (e: arrow) and cortical (g) plaques in APP/PS1

mice (29 weeks). In the same regions, iron labeling was diffuse in age-matched PS1 animals (f: subiculum (arrow), h: cortex). Scale bars: for a-d: 2 mm; for e-h: 500 µm.

Figure 4

Comparison between mean iron load and amyloid load in the parietal cortex (◊) and subiculum (♦) of APP/PS1 mice. Amyloid burden was significantly correlated to the iron load in the subiculum ($r=0.5$; $p<.05$) but not in the parietal cortex of APP/PS1 mice.

Figure 5

Correlation between T2 values and age in APP/PS1 (□, ——) and PS1 (■, ——) animals in the subiculum (a; $r=-0.57$, $p<.01$ for APP/PS1; $r=-0.74$, $p<.001$ for PS1), and the striatum (b; $r=-0.63$, $p<.001$ for APP/PS1; $r=-0.78$, $p<.001$ for PS1). The slopes of the regression curves fitting T2 values versus age was significantly greater in the subiculum of PS1 animals as compared to APP/PS1 mice (Student's t test, $p<.05$).

Figure 6

Comparison between T1 values and age in the striatum (a) and parietal cortex (b) of APP/PS1 (□, ——) and PS1 (■,——) animals. For the striatum, T1 values were correlated to age in APP/PS1 ($r=-0.74$, $p<.001$) and PS1 mice ($r=-0.71$, $p<.001$). The parietal T1 was significantly correlated to age only in APP/PS1 animals ($r=-0.65$, $p<.001$).

Figure 7

T2 values (mean± standard error of the mean) in the subiculum of adult and old animals. The T2 values were shorter in the subiculum of adult APP/PS1 (white boxes) animals as compared to age-matched PS1 mice (*: $p<.001$, $n_{APP/PS1}=10$ and $n_{PS1}=7$).

Table 1

Click here to download high resolution image

Table1

Figure 1
Click here to download high resolution image

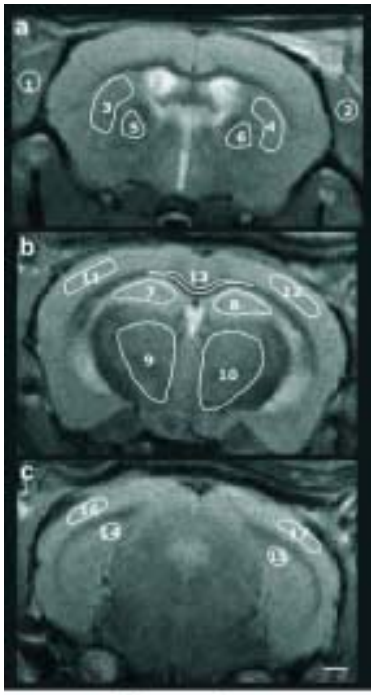

Figure 1

Figure 2
Click here to download high resolution image

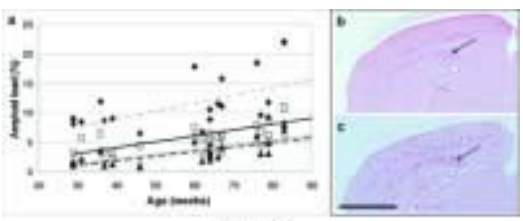

Figure 2

Figure 3
Click here to download high resolution image

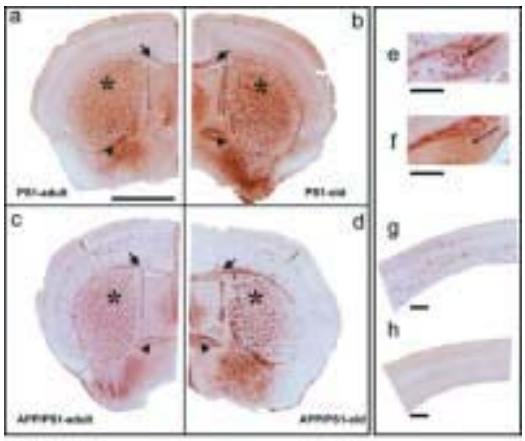

Figure 3

Figure 4
Click here to download high resolution image

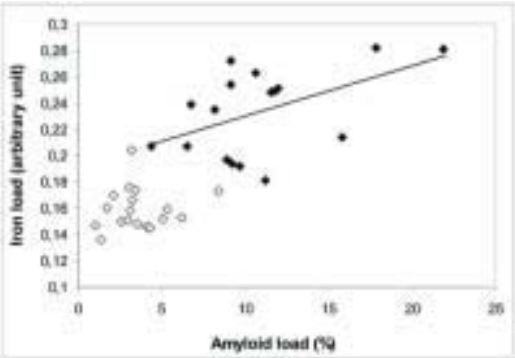

Figure 4

Figure 5
Click here to download high resolution image

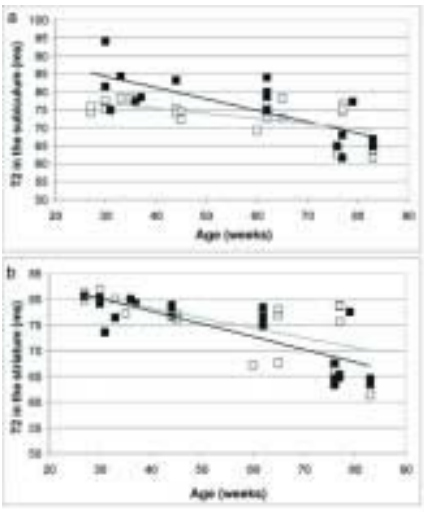

Figure 5

Figure 6

Click here to download high resolution image

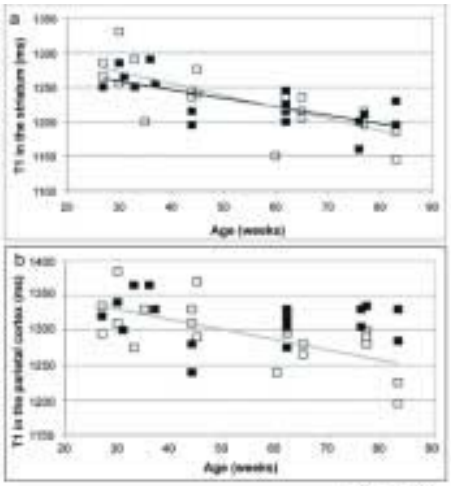

Figure 6

Figure 7
Click here to download high resolution image

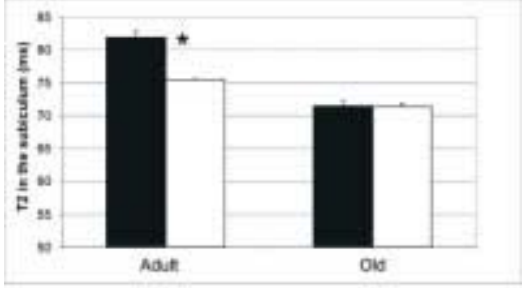

Figure 7